sciendo

INTERNATIONAL CONFERENCE enviBUILD BUILDINGS AND ENVIRONMENT 2019 7th November, Slovak University of Technology, Bratislava

STU SvF

CFD SIMULATION, CHANGE OF WIND VELOCITY THROUGH NETTING AS PERFORATED BARRIER

Jozef Bockaj [1] and Juraj Zilinsky [2]

[1] Department of Building Construction, STU Bratislava, Faculty of Civil Engineering, Radlinského 11, 813 68 Bratislava, Slovakia, Email: jozef.bockaj@stuba.sk

[2] Department of Building Construction, STU Bratislava, Faculty of Civil Engineering, Radlinského 11, 813 68 Bratislava, Slovakia, Email: juraj.zilinsky@stuba.sk

ABSTRACT

Main purpose of this article is determining the change in wind velocity and direction around and through the aerodynamic barrier. The barriers are made of four different types permeable materials and one barrier made of impermeable material. In the article is detailed description of the simulation procedure of the precise barriers in the program (CFD) Ansys Fluent 19.2.

The simulation of the particular barriers consists of determining the eligible size of the computational domain, which proposition was based on the connections with the barrier height, since the barrier width is negligible in this case. Choosing the suitable computational model for the simulation was important, especially being based on the Reynolds Averaged Navier-Stokes equations.

Based on the Forschheimer's equation, eligible positioning location of the aerodynamic barrier and adjustment for the permeability of individual materials in computer simulations.

Conclusion of this article is the evaluation of the aerodynamic barrier simulations with simple pointing at the speed changes and wind flow, around and through the aerodynamic barriers.

INTRODUCTION

The aerodynamic barriers divide the continuous flow area around the barrier into two principal parts. In the first part, in front of the barrier, windward area is formed (overpressure) and behind the barrier, leeward area (underpressure). The efficiency of reducing the flow rate and intensity of turbulence wind by the barrier is influenced by the following parameters: height, length, orientation, width, continuity, cross-section, permeability.

The main parameter of aerodynamic barriers is permeability (porosity or cross-section fullness) ϕ, which can be expressed as ratio between open parts area and total barrier area (expressed in m^2/m^2) [Jensen, 1954; Tillie, 1992].

Air flow and the change of the wind flow around solid obstacles has been as in the past also in the present time interesting area of research for many scientists such as Robertson [Robertson, 1996], Briassoulis [Briassoulis, 2010], Dong [Dong, 2010], Bailiang [Baliang, 2015] and others.

COMPUTER NUMERICAL SIMULATION

For the purpose of simulations of perforated (permeable) barriers the program ANSYS FLUENT 19.2 was used. ANSYS FLUENT is program based on the methods of finite volumes in three-dimensional

https://doi.org/10.2478/9788395669699-004

3D models, simulating fluid flow (in this case air) around specific barriers. In this case we examined air flow around the aerodynamic barrier, with height 2 m and length 4 m and with different material permeability. The thickness of the permeable barriers is actually very small and is between 0,2 - 0,8 mm.

For the permeability barrier simulation in ANSYS FLUENT, the parameters D and C_2 indicated in the equation (1) are essential, as well the parameters describing the permeable barrier α and β. If chosen the parameters α and β is possible to elect different thickness of the aerodynamic barrier Δx, taking in mind that the two-dimensional characteristics of the barrier will maintain. This implies that D and C_2 can be calculated with the equation (3). Even though the barrier thickness Δx while using the parameters α and β doesn't implements the aerodynamic barrier permeability of the mesh, the thickness can affect the air flow through and around the barrier. Based on this fact, the aerodynamic barrier thickness has to be thin compared to her height. That's why the aerodynamic barrier thickness is 20 mm which corresponds to the sides ratio (height/ thickness) equals to 100 [Agarwal, 2018].

The aerodynamic barriers were simulated as elevated above, the bottom surface of the computer 3D domains and wind flow perpendicular to the barrier plane. The size of the computational domain along the planes X, Y and Z was 40 m (20 h), 16 m (8 h), 14 m (7 h) (Fig. 3). The barrier was placed 12 m from the domain entry and 2 m height above the bottom surface of the computational domain. The domain size was chosen to fit to the height ratio of the barrier, since in this case has the main role for creating the windward and leeward barrier side. The barrier thickness is negligible. The domain size was considered so as to sufficiently eliminate the effects of air flow over the barrier on the windward and leeward side. The blockage ratio in the exposure plane was approximately 3,6 % [Agarwal, 2018].

In this article we are describing the simulations of five different aerodynamic barriers with different material permeability. Four aerodynamic barriers are simulated as permeable and one barrier as impermeable. The mesh of the final elements in the domain consist three-dimensional hexahedral elements for all barriers.

The barriers with permeable structure are discretized along the thickness of the barrier, and the impermeable barrier is modeled as impermeable wall and no elements were defined in the barrier volume. For creating the aerodynamic barrier computational mash, the use of hexahedral elements was inevitable. They were necessary to achieve the required convergence. In the computational domain with impermeable barrier fewer discretization elements were needed and used [Agarwal, 2018]. On the figure 2 we can see the disposition and the number of elements on the aerodynamic barrier surface. The amount of turbulence was higher in the areas of flow separation, that's why in the areas near the panel we needed to achieve a large number of elements. The zoomed part on the figure 2 shows detailed geometric characteristics of the orthogonal hexahedral elements placed along the panel thickness. The areas y - z from the front panel were evenly placed in square elements. The aerodynamic barrier was divided by height on 20 lines and 40 columns on width. For the accuracy of the simulations of permeable materials was necessary to create a finer mesh along the thickness of the barrier. The numerical simulation is more sensitive especially within the porous material and that's why five layers were formed along the barrier.

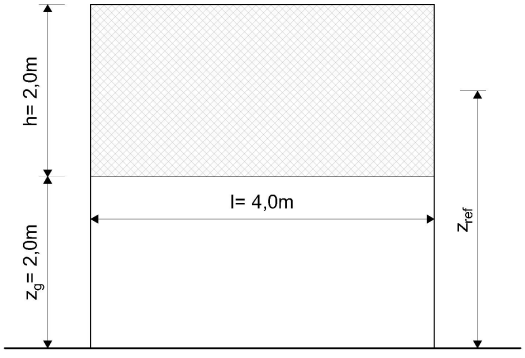

Figure 1. Dimensions of the simulated barrier.

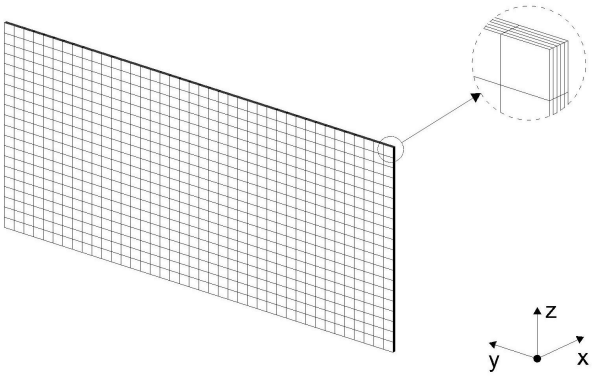

Figure 2. Dividing the computational elements on the barrier.

MODELING THE AERODYNAMIC BARRIER PERMEABILITY

The permeability of the aerodynamic barrier material was specified in the calculation based on the Forschheimer's equation [Paulotto, 2006]. This equation indicate the pressure loss Δp (N/m^2) through the porous material with thickness Δx (m).

$$\frac{\Delta p}{\Delta x} = \frac{\mu}{D} V + \frac{1}{2} C_2 \rho V^2 , \qquad (1)$$

where V - fluid velocity (m/s), μ - dynamic fluid viscosity (kg/m/s), ρ - fluid density (km/m^3), D - specific material permeability (m^2), C_2 - aerodynamic resistance coefficient (m^{-1}).

For thin panel with permeability:

$$\Delta p = \beta V + \alpha V^2 , \qquad (2)$$

$$\beta = \frac{\mu}{D} \Delta x, \quad \alpha = \frac{1}{2} C_2 \rho \Delta x , \qquad (3)$$

where α (Ns^2/m^4) and β (Ns/m^3) are the permeability characteristics and can be specified on the basis of measurements in the wind tunnel.

While simulating the aerodynamic barriers, four different materials were used with various porosity and one barrier made of impermeable material (Tab. 1). The table indicate the aerodynamic properties of the used materials. The values α and β express the permeability of the materials based on the experimental measurements in the wind tunnel [Hemming, 2005].

Permeable barrier		
Permeability (%)	Aerodynamic coefficient	
	α (Ns^2/m^4)	β (Ns/m^3)
38	3,02	0,12
46	0,79	0,86
54	0,94	0,3
62	0,36	0,5

Impermeable barrier		
Permeability (%)	Aerodynamic coefficient	
	α (Ns^2/m^4)	β (Ns/m^3)
0	-	-

Table 1. Barrier permeability with aerodynamic coefficients [Park, 2001].

MODELING THE TURBULENT STEAM IN SIMULATIONS

For the purposes of turbulent steam simulations through and around the barrier was used standard turbulent model k-ε and RNG k-ε. The standard model k-ε in most of the cases estimates turbulent kinetic energy. The given estimation usually happens during fluid flow around bluff bodies, where comes to significant changes in the speed gradient in the flow stream separation areas. Opposite of the k- model is the RNG k-ε model, which deals with the spread of kinetic energy turbulence more efficiently. Singular measure dispersion it's not assumed for all turbulence regardless to their size such as in the standard model k-ε, that's the reason why some of the turbulence are filtered [Agarwal, 2018].

In this case, we are no longer talking about permeable nets simulation but walls. We have added certain amount of permeability to the walls, based on the equation (1), and that's the reason why for this aim the computational model RNG k- has been selected.

CONDITIONS FOR WIND FLOW AND TURBULENCE

Speed profile given on the input to the computational area was set as logarithmical with computational wind speed V_z (m/s) with height z (m), given with the equation (4):

$$V_z = \frac{u_*}{K} ln\left(\frac{z+z_0}{z_0}\right), \qquad (4)$$

where z - reference height (m), V_z - wind speed at height z (m/s), u_* - internal friction speed (m/s), z_0 - surface roughness (m), K - von- Karman constant (≈ 0,41).

The inlet boundary conditions in the wind profile also contain turbulent wind characteristics k (m^2/s^2) and (m^2/s^3), which are given with the equations (5 and 6):

$$k = \frac{u_*^2}{\sqrt{C_\mu}}, \qquad (5)$$

$$\varepsilon = \frac{u_*^2}{K(z+z_0)}, \qquad (6)$$

where $C\mu$ - 0,09 is a constant from the k-ε model, u_* - is friction in the atmospheric boundary layer.

For the simulations of air flow in the modeled area is very important to consider the conditions related to air friction on the domain bottom surface (in this case the friction wasn't considered - smooth surface) (Wall boundary condition). As boundary conditions for the top and side surfaces were set domains without surface friction (Symmetry). On the output from the computational domain, was calculated with zero pressure and with that confirmed the open end rule (Outlet).

For individual wall barriers conditions were set on the surfaces related to porosity by using the parameters for web materials D and C2.

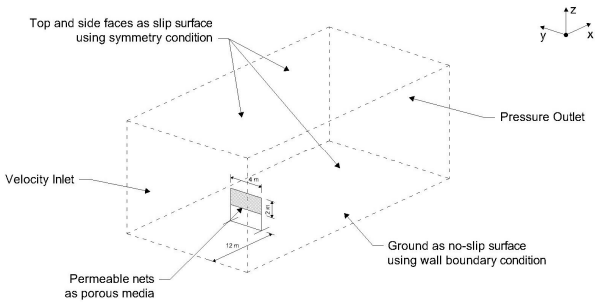

Figure 3. Placement the barrier in the computer domain.

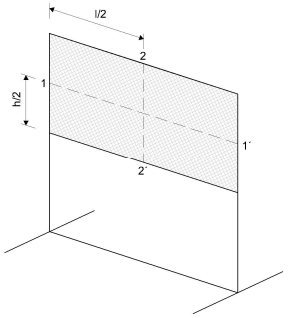

Figure 4. Scheme of the levels where wind speed was examined.

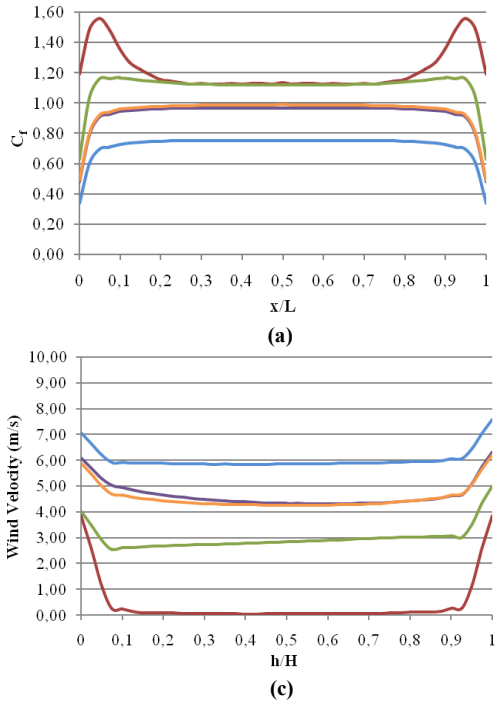

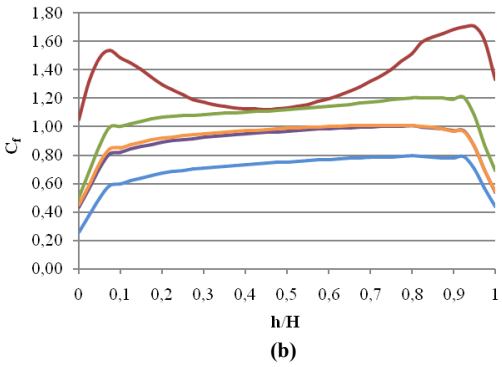

1. Impermeable barrier
2. Permeable barrier (38 %)
3. Permeable barrier (46 %)
4. Permeable barrier (54 %)
5. Permeable barrier (62 %)

C_f - pressure coefficient, expresses the efficiency and distribution of the wind load on the aerodynamic barrier surface

Figure 5. Simulation results

(a) Pressure coefficient C_f along barrier section 1-1 (analysis RNG k-ε).

(b) Pressure coefficient C_f by barrier height section 2-2 (analysis RNG k-ε).

(c) Velocity fluctuation by barrier height section 2-2 (analysis RNG k-ε).

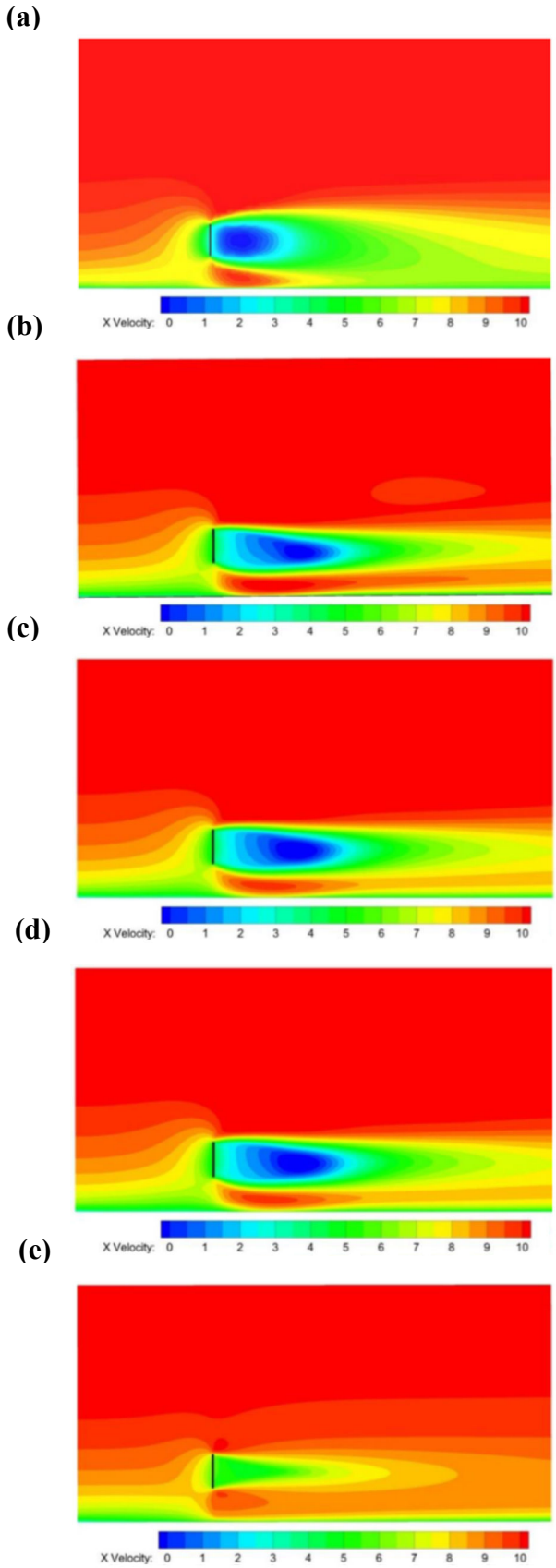

Figure 6. Illustration of the speed by barrier height section 2-2
(a) 1. Impermeable barrier (0 %)
(b) 2. Permeable barrier (38 %)
(c) 3. Permeable barrier (46 %)
(d) 4. Permeable barrier (54 %)
(e) 5. Permeable barrier (62 %)

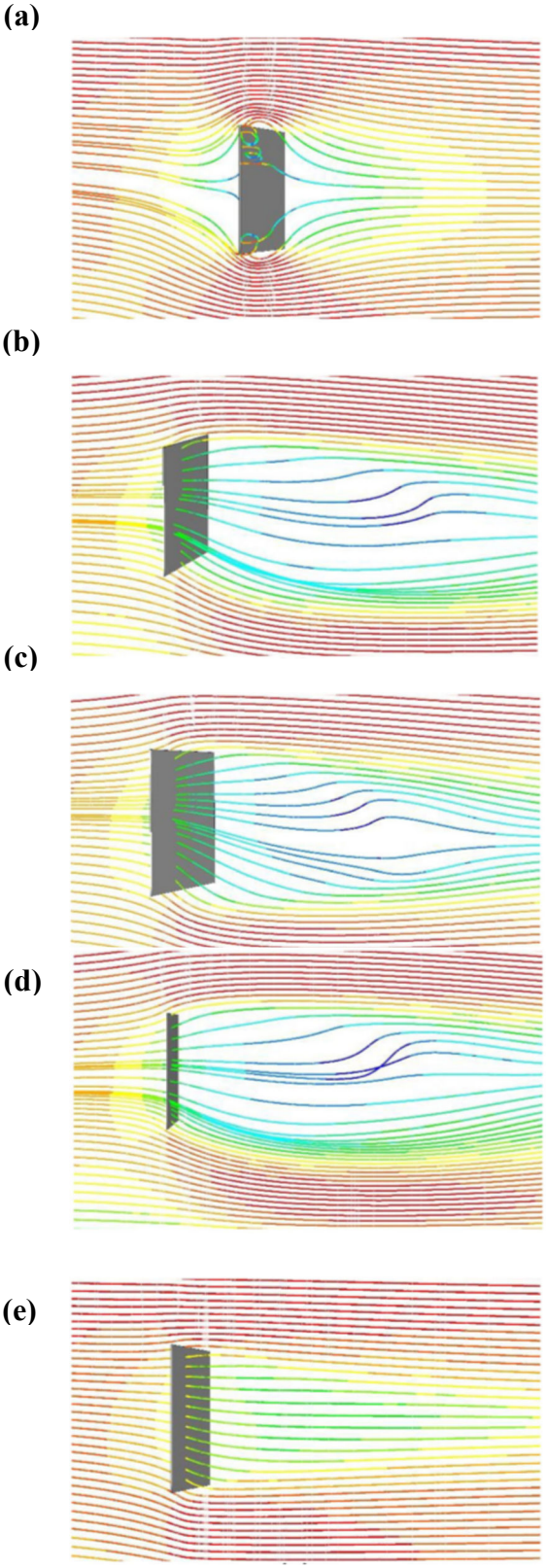

Figure 7. Trail of air flow by barrier height section 2-2
(a) 1. Impermeable barrier (0 %)
(b) 2. Permeable barrier (38 %)
(c) 3. Permeable barrier (46 %)
(d) 4. Permeable barrier (54 %)
(e) 5. Permeable barrier (62 %)

CONCLUSION

As a conclusion we can evaluate and assume that the aerodynamic barriers made of perforated materials efficiently eliminate the wind flow velocity in the areas in front and behind the barrier. In this article are described simulations of aerodynamic barriers from impermeable and permeable materials based on the Forschheimer's equation, which specifies loss of air pressure through the barrier.

We need to take in considerations that the consistency of the simulations made in the program with specified permeability based on the the Forschheimer's equation compared with the simulations of the barrier as mesh (without using the equation for pressure loss) is questionable. As an example is the comparison of the aerodynamic barrier simulation with permeability 50 % and individual openings with dimensions 2 x 2 mm and aerodynamic barrier simulation with equal permeability but with individual openings with dimensions 20 x 20 mm.

Shouldn’t be forgotten that in case of simulations of very fine mesh materials is necessary to meet the conditions for minimum number of computational cells on the barrier surface in each opening (minimum 9 cells), which in this case is very demanding for the computational technology.

ACKNOWLEDGEMENT

This article was created with the support of the Ministry of Education, Science, Research and Sport of the Slovak Republic within the Research and Development Operational Programme for the project "University Science Park of STU Bratislava", ITMS 26240220084, co-funded by the European Regional Development Fund.

REFERENCES

[1] Jensen M., 1954, *Shelter Effect: Investigations into Aerodynamics of Shelter and its Effects on Climate and Crops*, Danish Tech, press, Copenhagen.

[2] Tillie M., 1992, *Ambiance dans les batimentsd´élevagebovin*, Session Institut de l´Elevage, No. 222, Paris.

[3] Robertson A. P., et. al., 1996, *Full-scale testing to determine the wind loads on free-standing walls*, Journal of Wind Engineering and Industrial Aerodynamics, 60, p. 123-137.

[4] Briassoulis D., et. al., 2010, *Wind forces on porous elevated panels*, Journal of Wind Engineering at Industrial Aerodynamics, 98 , p. 919-928.

[5] Dong Z., et. al., 2010, *A wind tunnel simulation of the turbulence fields behind upright porous wind fences*, Journal of Arid Environments, 74, p. 193-207

[6] Bailiang L., et. al., 2015, *Aerodynamics and morphodynamics of sand fences: A review*, Aeolian Research, 17, p. 33-48.

[7] Agarwal A., et. al., 2018, *Numerical Investigation of the Turbulent Wind Flow Through Elevated Windbreak*, Journal of The Institution of Engineers (India): Series, 99, p. 311-320.

[8] Paulotto C., et. al., 2006, *Wind tunnel evaluation of mean wind pressure on a frame-type signboard*, Journal of The Institution of Engineers (India): Series, 98, p. 919-928.

[9] Hemming S., et. al., 2005, *Testing of air permeability performance of agricultural nets*, in Internal Report, *Agrotechnology and Food Innovations*, ed. By B.V Wageningen, U.R. Wabgeningen (The Netherlands, 2005).

[10] Park C. W., et. al., 2001, *The effects of a bottom gap and non-uniform porosity in a wind fence on the surface pressure of a triangular prism located behind the fence*, Journal of Wind Engineering at Industrial Aerodynamics, 89, p. 1137-1154.